Initial Observations on the Burning of an Ethanol Droplet in Microgravity

$$\sum \dot{\omega}_i H_i$$

$$\nabla \cdot q_R$$

Andrei Kazakov, Bradley Urban, Jordan Conley and Frederick L. Dryer

Department of Mechanical and Aerospace Engineering
*Princeton University*
Princeton, New Jersey 08544-5263

Motivation

droplet studies in microgravity:

- simple geometric configuration - opportunity for testing/validating theory

- facile method to study the diffusive combustion of fuel molecular species similar to those in transportation fuels

- link to multi-droplet (spray) applications
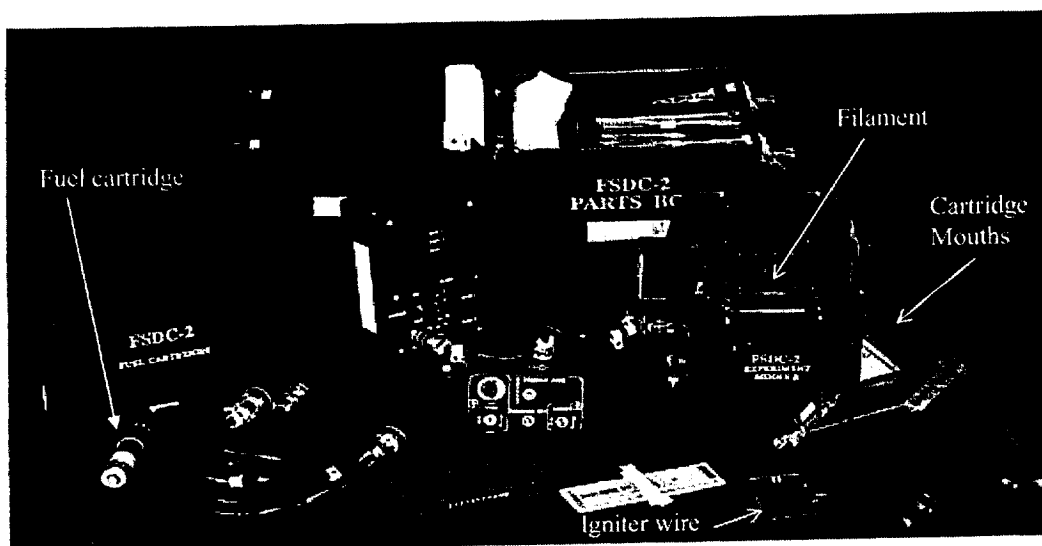
- fire safety criteria in space

ethanol:

- relatively simple and established chemistry

- azeotropic behavior of mixtures with water

- change in sooting tendency with pressure

- important gasoline fuel additive
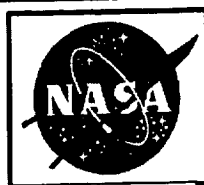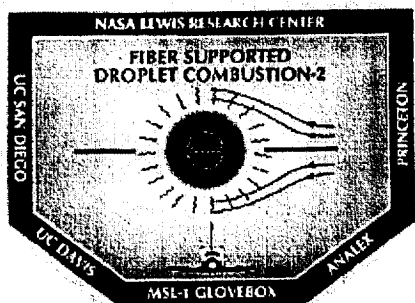
Fiber Supported Droplet Combustion
FSDC-2
MSL-1/STS-94 (July 1997)

- Drops tethered on silicon-carbide fibers (80, 150 microns), 2 to 5 mm initial diameter.

- Fuels: Methanol, Methanol-Water, **Ethanol**, n-Heptane, n-Decane, n-Heptane-Hexadecane.

- Burned in cabin air (1 atm, 22-25 C, 39-46% RH)

- Quiescent (all), convective (n-Heptane, n-Decane), & multiple drop (n-Heptane, n-Decane) experiments

- Backlighted drop, direct flame video, & dual radiometer measurements.

Droplet burning history

pure ethanol, $d_0 = 3.41$ mm
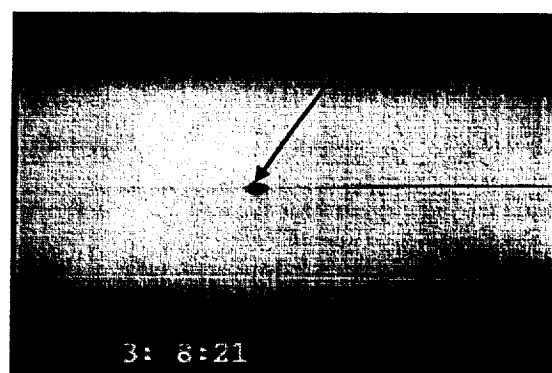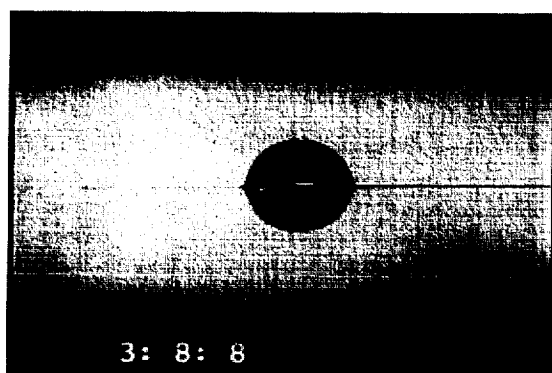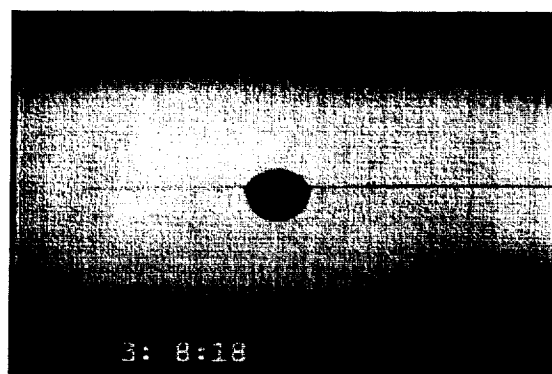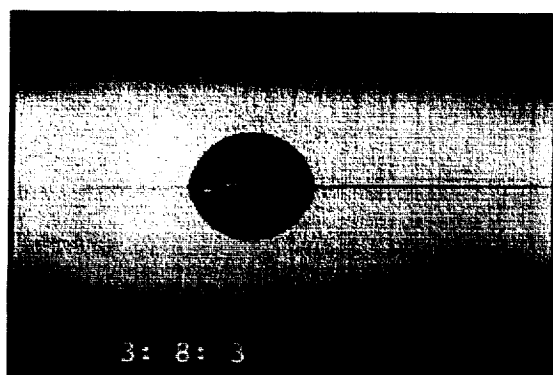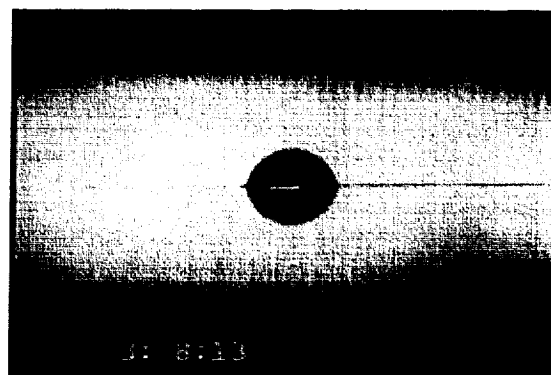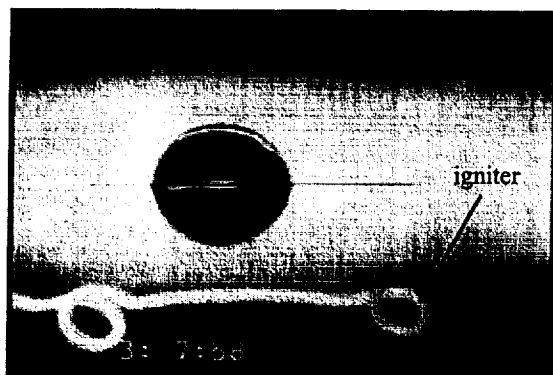
Data reduction
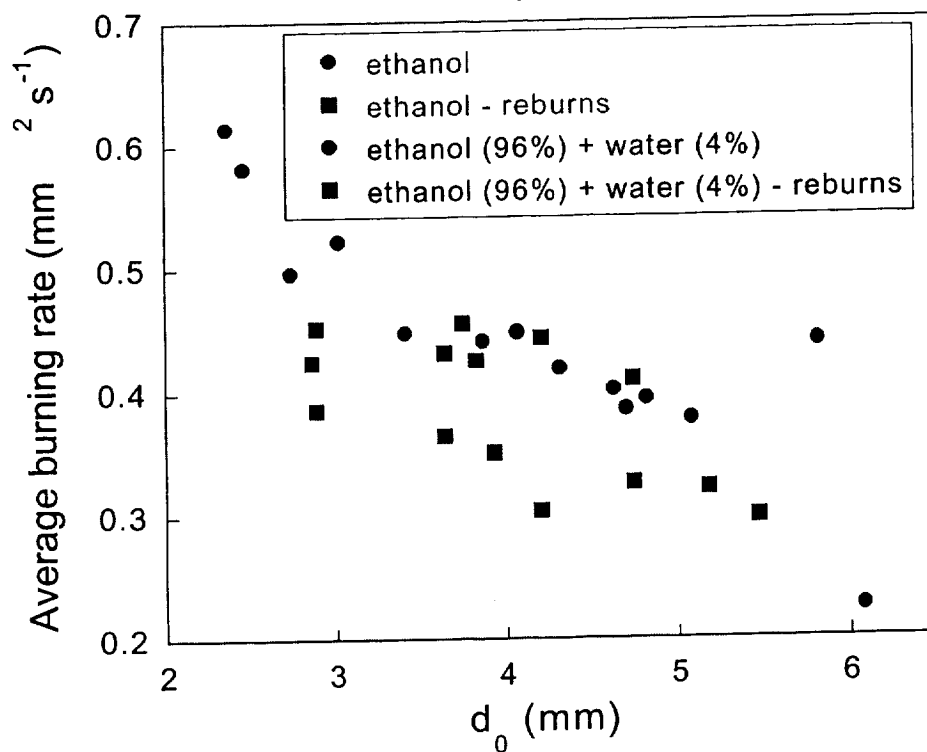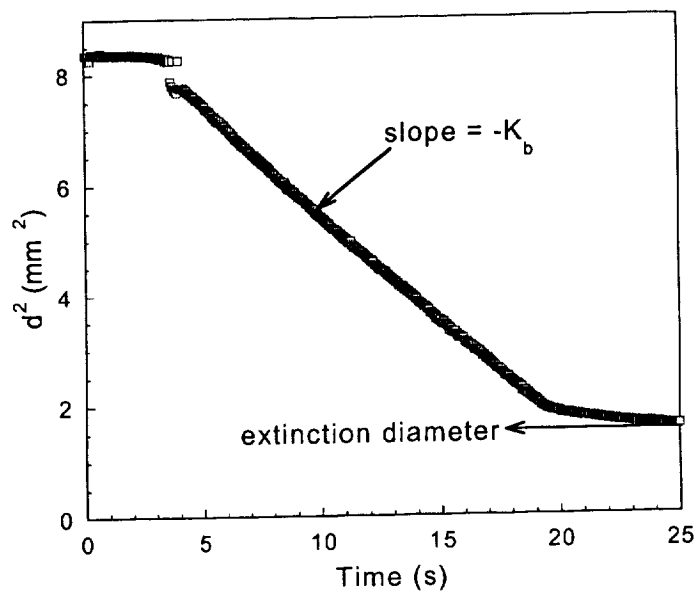
Data reduction (cont'd)

Ethanol droplet extinction diameter
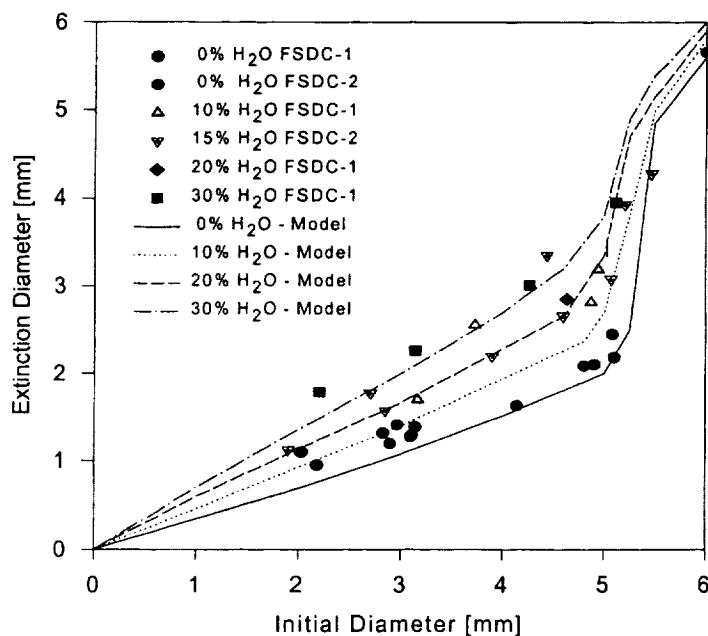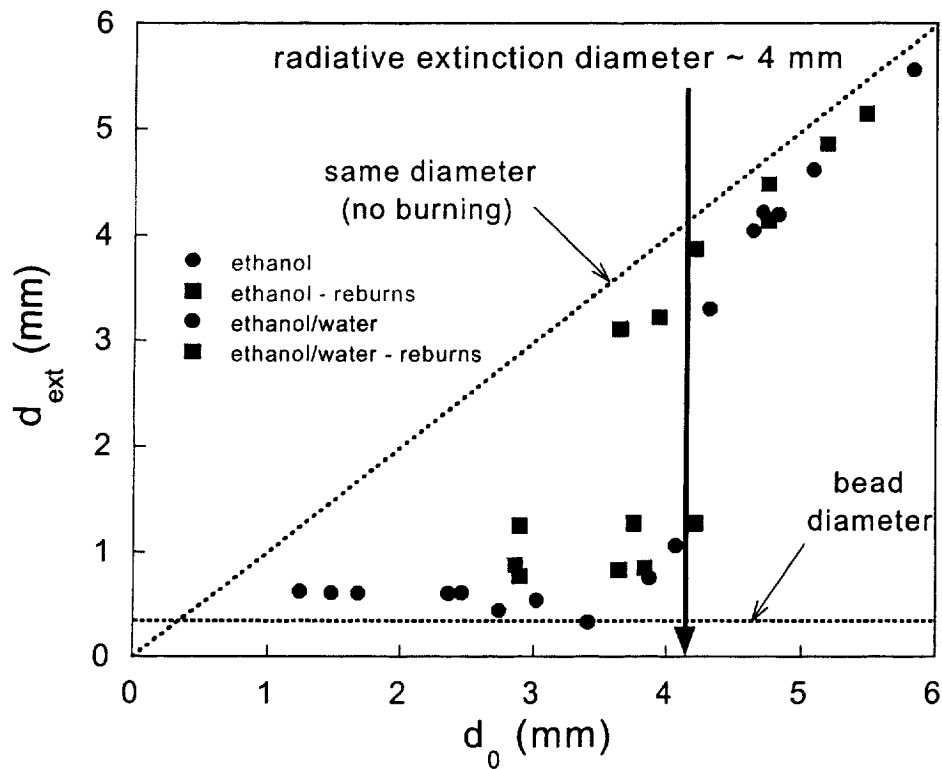
Methanol data
Marchese&Dryer (1999)

Time-Dependent, Spherically Symmetric, Bi-component Model for Droplet Combustion

(Based on FEM approach of Cho, et al., 1992)

Gas Phase:
- Multicomponent molecular diffusion
- Detailed chemical kinetics
- Spectral (non-luminous) thermal radiation
- UV flame emission

Mass Conservation:

$$\frac{\partial}{\partial t}(\rho_g) + \frac{1}{r^2}\frac{\partial}{\partial r}(r^2\rho_g v) = 0$$

Species Equations:

$$\frac{\partial(\rho_g Y_{g,i})}{\partial t} + \frac{\partial(\rho_g Y_{g,i})}{\partial r} = -\frac{1}{r^2}\frac{\partial}{\partial r}(r^2\rho_g Y_{g,i} V_{r,i}) + \omega_{g,i}$$

Energy Conservation:

$$\frac{\partial(\rho_g C_{p,g} T_g)}{\partial t} + v_r \frac{\partial(\rho_g C_{p,g} T_g)}{\partial r} = \frac{1}{r^2}\frac{\partial}{\partial r}\left(r^2(\lambda_g \frac{\partial T_g}{\partial r} - q_R)\right)$$

$$- \sum_{i=1}^{n} \frac{\partial \rho_g (Y_{g,i} V_{r,i} C_{p,g,i}) T_g}{\partial r} - \sum_{i=1}^{n} \omega_{g,i} H_{g,i}$$

Droplet Surface:
- Surface regression
- Evaporation of fuel
- Condensation/Dissolution of products
- Radiative heat exchange

Net Radiative Heat Flux

$\dot{m}_v$

$\dot{m}_p$

q_R

$D_{l,i}\frac{\partial Y_{l,i}}{\partial r}$

$\lambda_L \frac{\partial T}{\partial r}$
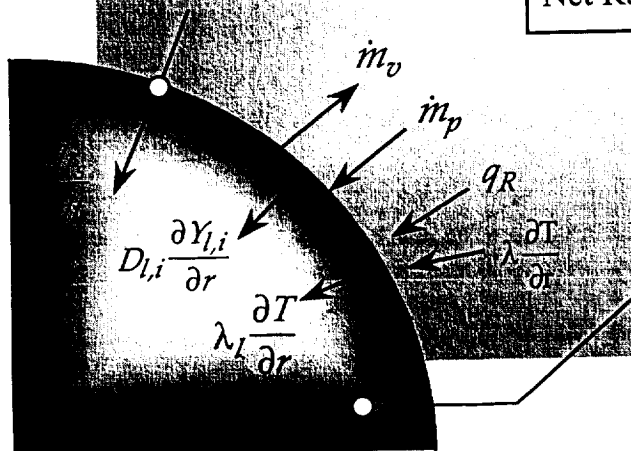
Droplet Interior:

$$\frac{\partial(\rho_l C_{p,l} T_l)}{\partial t} = \frac{1}{r^2}\frac{\partial}{\partial r}\left(r^2\lambda_l \frac{\partial T_l}{\partial r}\right)$$

$$\frac{\partial Y_{l,i}}{\partial t} = \frac{1}{r^2}\frac{\partial}{\partial r}\left(r^2 D_{l,i}\frac{\partial Y_{l,i}}{\partial r}\right)$$

Model: further details

- detailed reaction mechanism of C_2H_5OH oxidation (Norton&Dryer, 1992)
  - 33 species
  - 142 reversible elementary reactions
- molecular transport parameters (CHEMKIN database & estimates)
- ethanol/water vapor pressure correlations (Kurimara et al. 1995)
- improved non-luminous radiation model

Vaporization of suspended ethanol droplets in dry and humid air ($d_0 = 1.6$ mm, $T_0 = 297$ K)

Law et al. (1987) - 100% humidity

Law et al. (1987) - dry
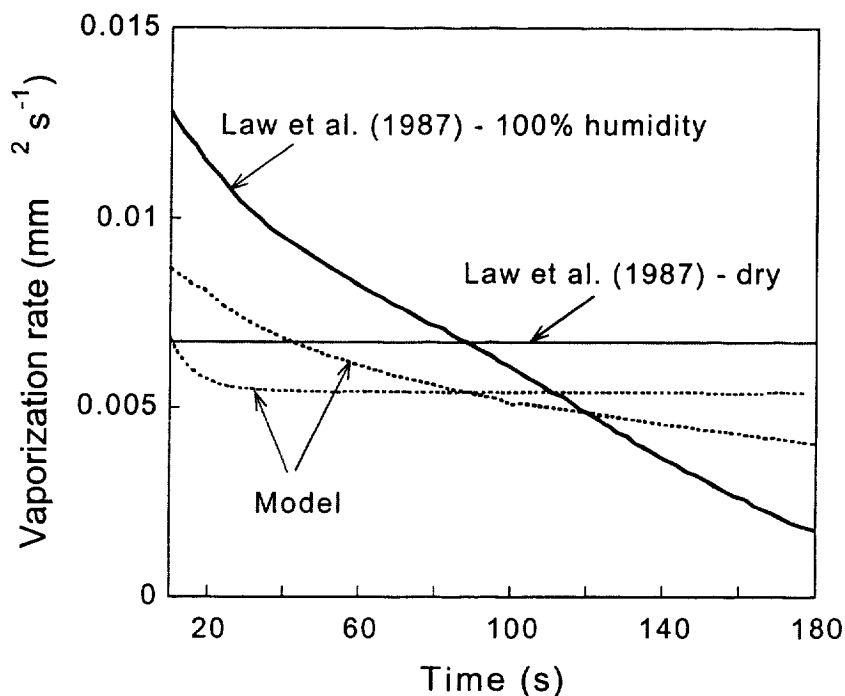
Model

Preliminary Modeling Results

Ethanol droplet combustion, $d_0 = 1$ mm, 1 atm, 298 K
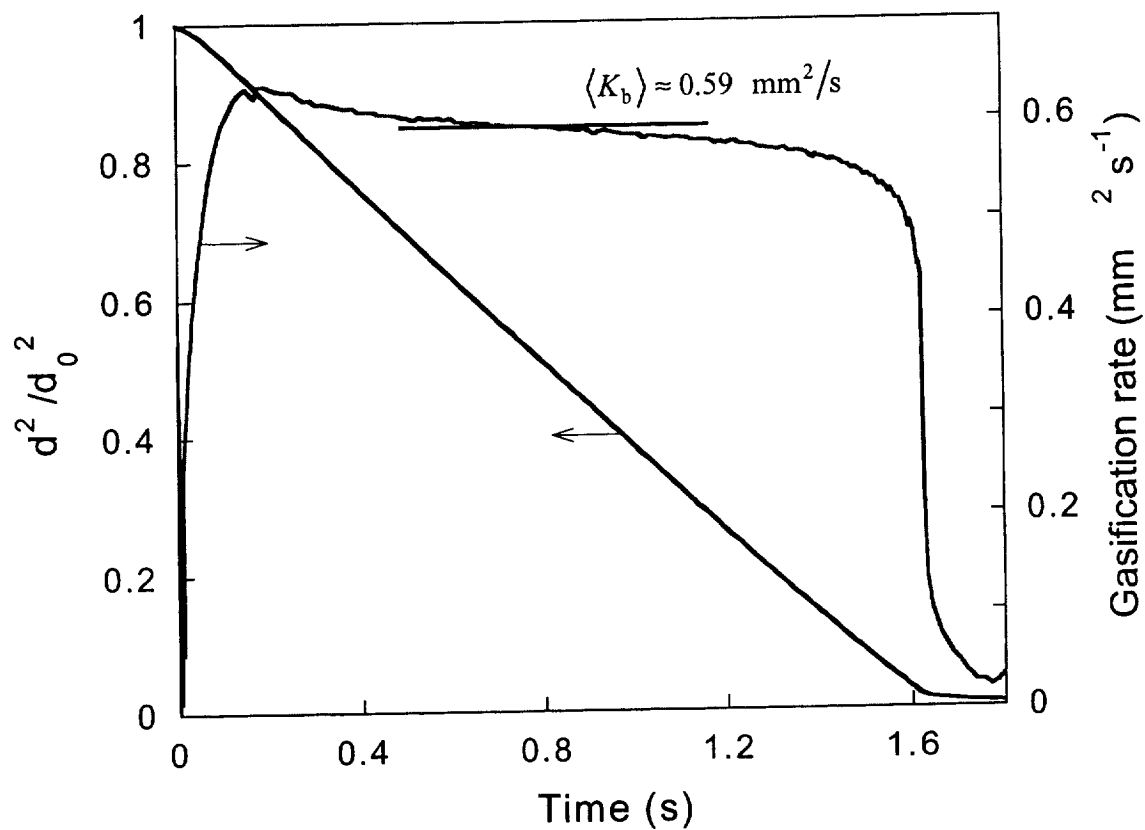
consistent with experimental data:

- closely follows d^2-law during most of its burning history
- very small extinction diameter

Preliminary Modeling Results (cont'd)
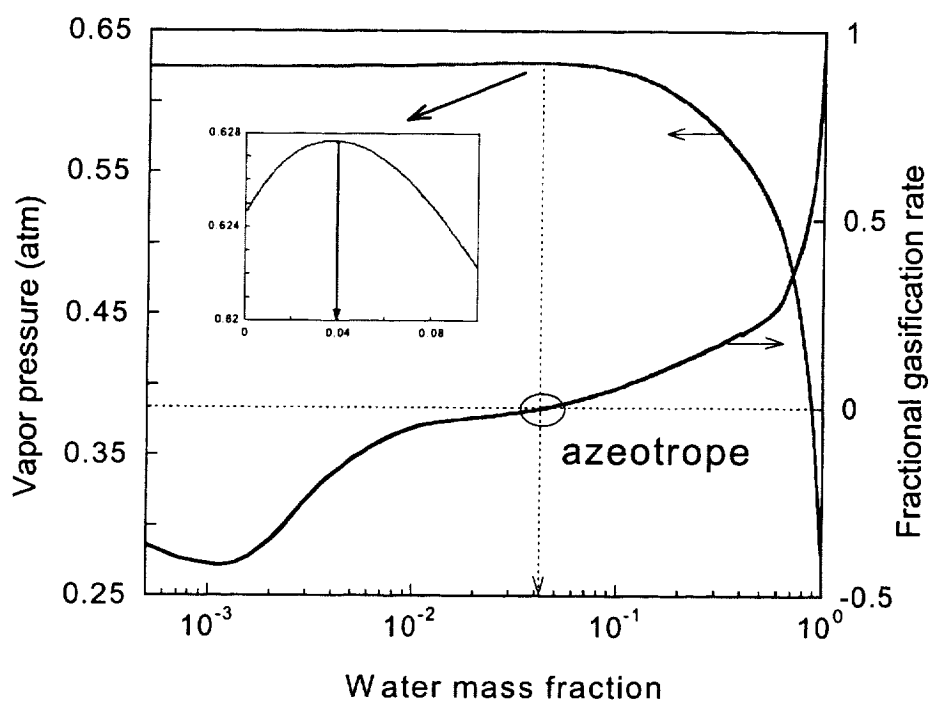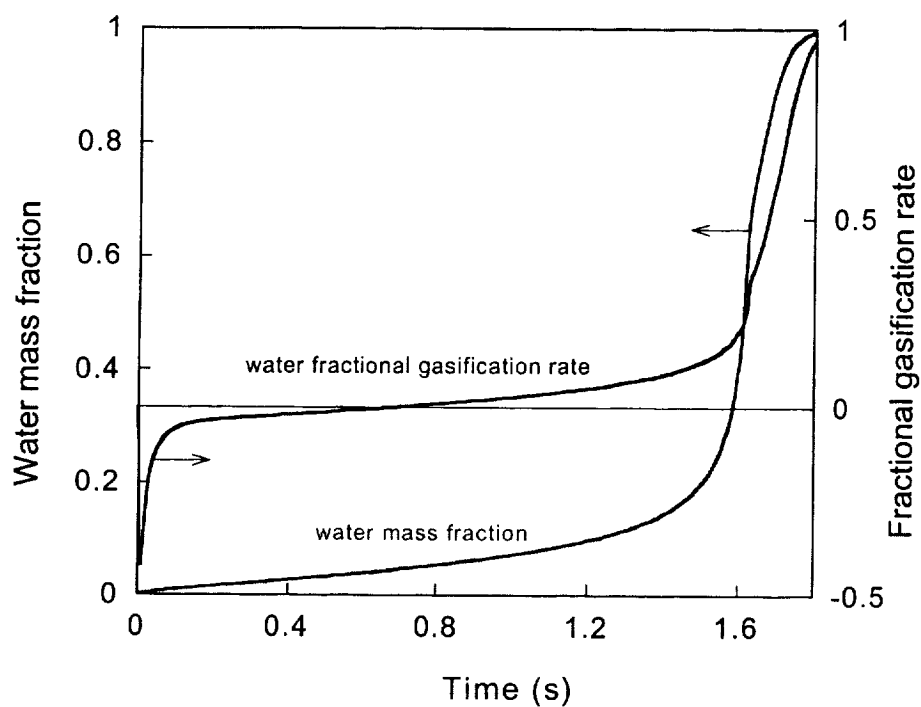
Summary

•first experimental information on ethanol droplet burning in microgravity
- burning rates
- extinction diameters
- radiative extinction diameter (~ 4 mm)
- flame diameters

•ethanol droplet combustion is less influenced by water condensation as opposed to previously studied methanol cases

•preliminary computational analysis is in consistence with experimental findings

•further computational analysis is in progress; additional experimental work (FSDC-3) is planned

Acknowledgements

Extras follow…

From Struk et al. (1998)
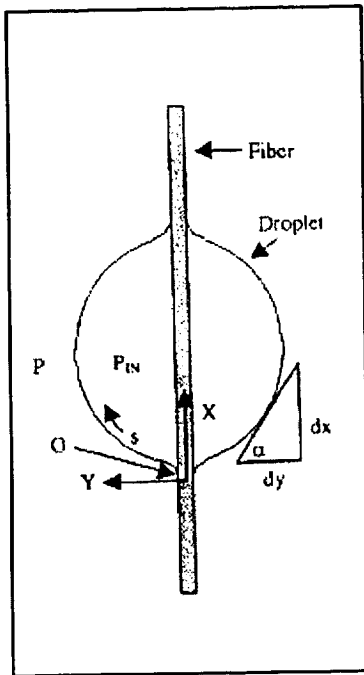
Geometry of a droplet
on fiber in microgravity

Simulated burning with
pre-assigned burning
constant
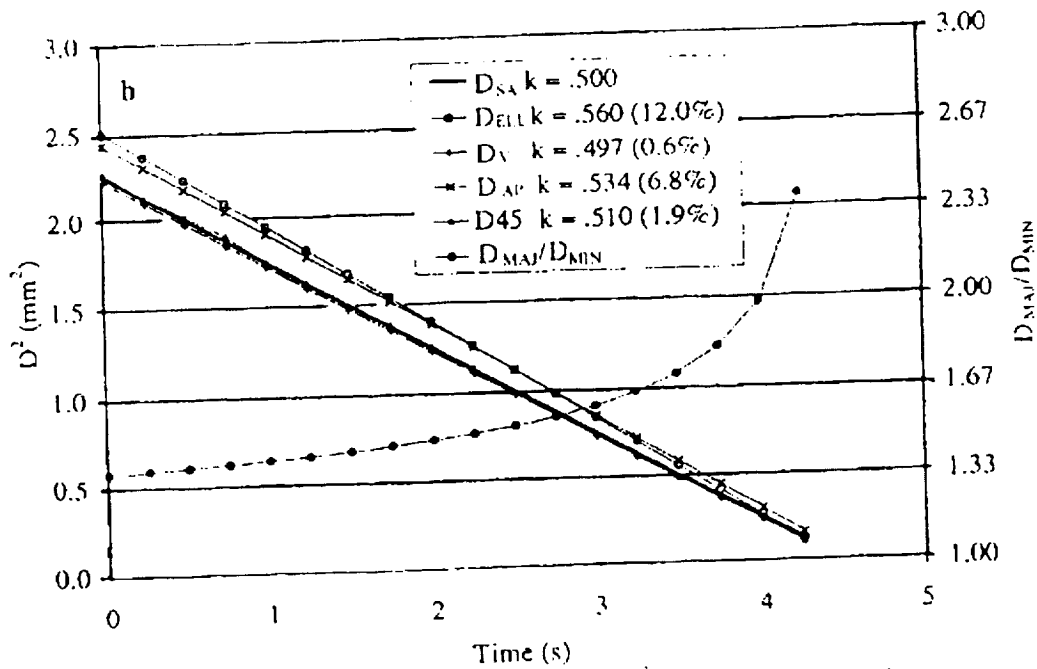
Flame Standoff

Pure ethanol, $d_0 = 2.89$ mm
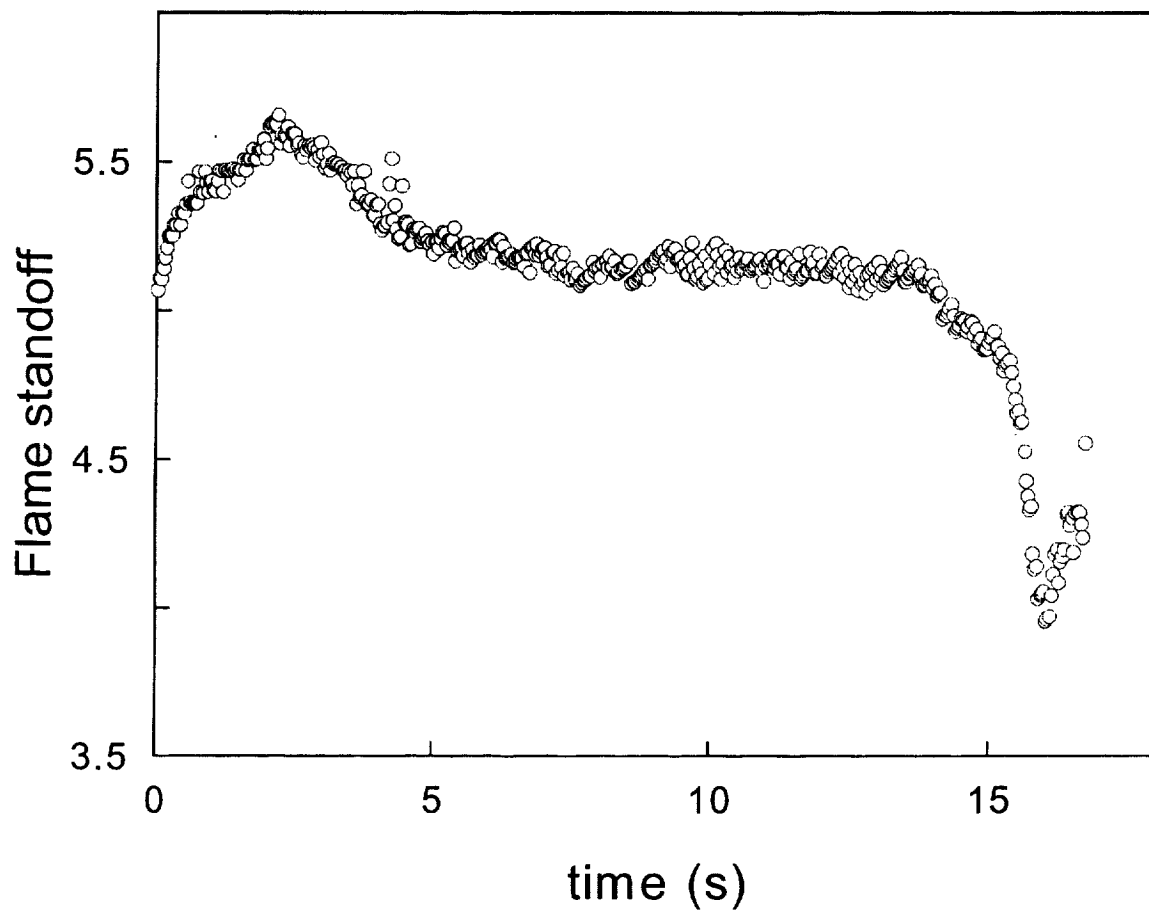
Initial Observations on the Burning of an Ethanol Droplet in Microgravity

Andrei Kazakov, Bradley Urban, Jordan Conley and Frederick L. Dryer

Department of Mechanical and Aerospace Engineering,
Princeton University, Princeton, NJ 08544

INTRODUCTION

Combustion of liquid ethanol represents an important system both from fundamental and practical points of view. Ethanol is currently being used as an additive to gasoline in order to reduce carbon monoxide and particulate emissions as well as to improve the fuel octane rating. A detailed physical understanding of liquid ethanol combustion is therefore necessary to achieve an optimal performance of such fuel blends in practical conditions. Ethanol is also a relatively simple model compound suitable for investigation of important combustion characteristics typical of more complex fuels. In particular, ethanol has been proposed for studies of sooting behavior during droplet burning [1]. The sooting nature of ethanol has pressure sensitivities similar to that of n-heptane, but shifted to a higher range of pressures (1-3 atm). Additionally, liquid ethanol is miscible with water produced during its combustion forming mixtures with azeotropic behavior, a phenomenon important for understanding multi-component, liquid fuel combustion [2]. In this work, we present initial results obtained in the series of recent space-based experiments [3] and development a detailed model describing the burning of ethanol droplet in microgravity.

EXPERIMENTAL

The microgravity ethanol droplet combustion experiments were performed aboard the STS-94/MSL-1 Shuttle mission within the Fiber-Supported Droplet Combustion-2 (FSDC-2) program [3]. All experiments were carried out in the Glovebox (MGBX) facility using the FSDC-2 experimental apparatus. Ethanol and ethanol/water mixtures were contained in modified, airtight commercial syringe cartridges. To operate the experiment, the fuel cartridge was screwed into the base of the experiment module. The crew turned a plunger screw, forcing fuel through two, opposed, hypodermic needles to the deployment site on a silicon fiber located between the needles and perpendicular to them. After the fuel coalesced into a droplet of the desired size, the needles were slowly retracted to minimize contact of the liquid with the needle surfaces. The stretched droplet was then deployed by rapidly retracting the needles into the bottom of the chamber. Motions of the deployed droplet were allowed to dampen before the ignition button was depressed. This automatically lifted a replaceable igniter wire into place on one side of the droplet (parallel to the fiber), approximately 3.5 mm from the fiber, and simultaneously provided DC electric current to the igniter. When the crew operator detected ignition visually, the igniter button was released, automatically retracting the igniter to the bottom of the test chamber. The manual nature of the experiment can affect the reproducibility and fidelity of the data, in comparison to that obtained in the full-facility Droplet Combustion Experiment (DCE) apparatus. However, FSDC experiments provide substantial scientific insights as well as first-order data on which to base more refined DCE studies.

Imaging data are provided by two video views, one a backlit view of the droplet and the other a perpendicular view of the flame. The video camera for the droplet view was attached to the Glovebox microscope. The second video camera, with a view essentially orthogonal to the microscope, recorded the droplet, the fiber, and the flame. All of the data were recorded using three 8 mm VCR's. The taped camera images were analyzed using microcomputer-based imaging analysis systems. Each droplet combustion test occurred at pressures (0.996–1.107 bar), oxygen mole fractions (0.204–0.222), and relative humidity (39–46%) of the Spacelab environment.

The average droplet gasification rate, $K = d(d_s^2)/dt$, where d_s is an instanteneous droplet diameter, and t the burning time, for pure ethanol and ethanol/water mixtures, as a function of initial droplet size, are presented in Figure 1. The results show that average gasification rate is related to the initial droplet size in a manner similar to n-alkanes and methanol [4-6] and consistent with ethanol data taken recently in the NASA-Lewis 2.2 s droptower [7]. The FSDC-2 ethanol experiments were particularly interesting in that large initial droplets that burned unsteadily and underwent extinction could be re-ignited. The gasification rate of the re-ignited droplet was typically higher in comparison to the prior burn. Larger initial droplet sizes could be re-ignited several times. Eventually, the re-ignited droplets would burn in a sustained fashion to near completion (an extinction diameter that was not measurable). Further data reduction and analyses, complemented by computer simulations are currently in progress.

MODELING

A transient, moving finite-element chemically reacting flow model developed by Cho et al. [8,9] and applied previously to sphero-symmetric combustion of methanol [4], methanol/water [4,5], n-alkane, and n-alkane binary mixture [6] droplets was adopted for the problem of ethanol droplet combustion. The model includes detailed description of gas-phase reaction chemistry and transport, a simplified description of liquid phase transport, and non-luminous radiation [10].

Gas-phase chemistry was described with the detailed reaction mechanism of Norton and Dryer [11], which consists of 142 reversible elementary reactions of 33 species. Another recently published reaction mechanism of high-temperature ethanol oxidation [12] is also under consideration. However, our preliminary comparison of two reaction models using a representative opposite-flow diffusion flame problem [13] indicates that the basic flame structures predicted by these models are very similar. Large differences appear in profiles of primary pyrolysis products, particularly ethylene and acetaldehyde. The mechanism of Marinov [12] strongly emphasized thermal decomposition of ethanol, in comparison to abstraction channels. Other kinetic studies to experimentally characterize ethanol pyrolysis at near 1000 K are underway in this laboratory. The equilibrium vapor pressures for binary ethanol/water mixtures needed to define the boundary conditions on gas-liquid interface were evaluated using recently reported empirical correlations of Kurihara and co-workers [14]. The mixture liquid densities were computed using the excess-volume data of Bai et al. [15] and the correlations for pure compounds complied by Daubert and Danner [16].

The model predictions for 1 mm ethanol droplet burning in air at 1 atm are presented in Figs 2 and 3. As can be seen, the droplet size history fairly closely follows the classical d^2-law [16] with an average gasification rate constant of about 0.58 mm^2 s^{-1} which compares favorably with the experimental data presented in Fig. 1. This observation also differs from the experimental and numerical results obtained for methanol droplets that have shown significant deviations from the d^2-law predictions due to substantial water accumulation in the liquid phase [6]. As shown in Fig. 3, the model predicts relatively small mass fraction of water present in the ethanol droplet during most of the droplet lifetime, hence, the effect of water condensation on gasification rate is reduced as compared to the methanol cases. Furthermore, the water fractional gasification rate changes its sign relatively early during the process, indicating that condensation of water ceases, and the subsequent increase in water mass fraction in the droplet is caused exclusively by preferential gasification of ethanol. Similar conclusions can be drawn from the analysis of the experimental data for ethanol reported by Lee and Law [18]. Lee and Law have suggested that the observed difference in water condensation between methanol and ethanol droplets is primarily caused by a higher latent heat value of ethanol (9.7 kcal/mol) as opposed to the one of methanol (8.4 kcal/mol). Numerical tests performed in the present study indicated that reducing the latent heat of ethanol to the value of methanol without changing the vapor pressure relationships does not result in significant changes in calculated droplet water content during most of the process. A more detailed

analysis of model predictions reveals that water condensation stops approximately when the droplet composition reaches azeotropic point corresponding to about 4 % of water by mass. By definition, this composition occurs at the maximum of total vapor pressure (Fig. 4). Further increase of water content in the liquid phase leads to the decrease in total vapor pressure, and the subsequent condensation of water vapor becomes unfavorable.

A significant increase in water content in the droplet occurs late in the computed burning history. This observation has not been reported previously and is due to the non-ideal nature of the binary mixture vapor pressure/mass fraction relationship [14] (see Fig. 4).

SUMMARY

New experimental data for the ethanol droplet combustion in microgravity are presented. The reported values of average gasification rate are consistent with available literature trends and preliminary modeling results. The model analysis also indicates that water condensation in the case of ethanol has a smaller effect on droplet gasification rate as compared with previously studied methanol cases. Further analysis of experimental data and model development and validation are currently in progress.

ACKNOWLEDGMENTS

REFERENCES

1. Manzello, S. L., Hua, M., Choi, M. Y., and Dryer, F. L. "Experiments and Model Development for Investigation of Sooting and Radiation Effects in Microgravity Droplet Combustion", Proceedings of the Fifth International Microgravity Combustion Workshop, Cleveland, Ohio, May 18-20, 1999, p. 241.
2. Kim, J. S., Lee, A., and Law, C. K., *Twenty-Third Symposium (International) on Combustion*, The Combustion Institute, Pittsburgh, PA, 1990, p. 1423.
3. Colantonio, R., Dietrich, D., Haggard, J. B., Jr., Naygan, V., Dryer, F. L., Shaw, B. D., and Willams, F. A., "Fiber Supported Droplet Combustion-2", Proceedings of the Microgravity Science Laboratory One Year Science Review Meeting, Huntsville, Alabama, August 25-26, 1998, p. 141.
4. Marchese, A. J., Dryer, F. L., Colantonio, R., and Naygan, V. *Twenty-Sixth Symposium (International) on Combustion*, The Combustion Institute, Pittsburgh, PA, 1996, p. 1209.
5. Marchese, A. J., and Dryer, F. L. *Combust. Flame,* 105:104-122 (1996).
6. Marchese, A. J., Dryer, F. L., and Naygam, V. *Combust. Flame*, 116:432-459 (1999).
7. Colantonio, R., and Naygan, V., "Radiative Heat Loss Measurements during Microgravity Droplet Combustion", Proceedings of the 1997 Central States Section of the Combustion Institute.
8. Cho, S. Y., Yetter, R. A., and Dryer, F. L., *Mathl Comput. Modeling*, 14:790-794 (1990).
9. Cho, S. Y., Yetter, R. A., and Dryer, F. L., *J. Comp. Phys.*, 102:160-179 (1992).
10. Marchese, A. J., and Dryer, F. L. *Combust. Sci. Technol.,* 124:371-401, 1997.
11. Norton, T. S., and Dryer, F. L., *Int. J. Chem. Kinetics*, 24:319-344 (1992).
12. Marinov, N. M., *Int. J. Chem. Kinetics*, 31:183-220 (1999).
13. Lutz, A. E., Kee, R. J., Grcar, J. F., and Rupley, F. M. *OPPDIF: A Fortran Program for Computing Opposed-Flow Diffusion Flames*, Sandia National Lab Report No. SAND96-8243, 1997.
14. Kurihara, K., Minoura, T., Takeda, K., and Kojima, K., *J. Chem. Eng. Data*, 40:679-684 (1995).
15. Bai, T.-C., Yao, J., and Han, S.-J., *J. Chem. Thermodynamics*, 30:1347-1361 (1998).
16. Daubert, T. E., and Danner, R. P. *Physical and Thermodynamic Properties of Pure Chemicals: Data Compilation*, Hemisphere, New York, 1989.
17. Godsave, G. A. E. *Fourth Symposium (International) on Combustion*, The Combustion Institute, Pittsburgh, PA, 1953, p. 818; Spalding D. B. *Fourth Symposium (International) on Combustion*, The Combustion Institute, Pittsburgh, PA, 1953, p. 847.
18. Lee, A., and Law, C. K. *Combust. Sci. Technol.*, 86:253-265 (1992).
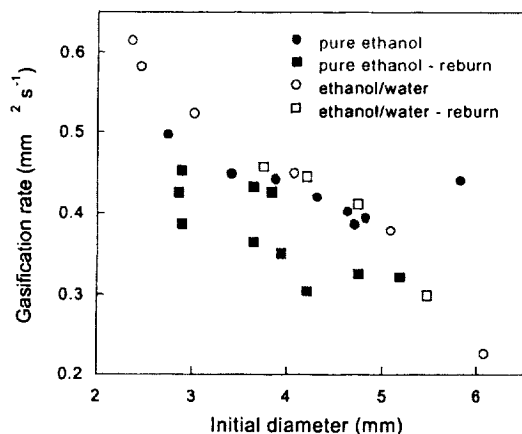
Figure 1. Average gasification rate constant as a function of initial droplet diameter for ethanol droplet burning in air [3].
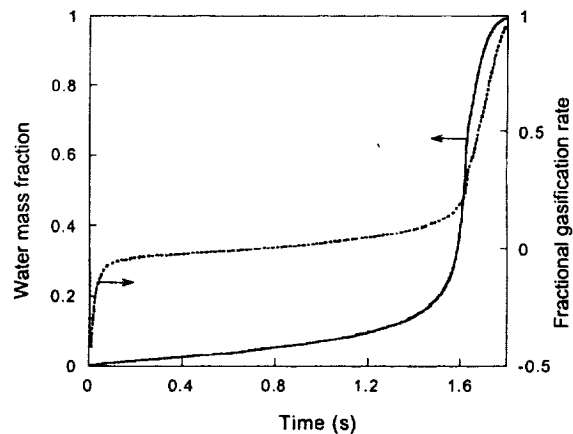

Figure 3. Water mass fraction (solid line) and fractional gasification rate, $\dot{m}_{H_2O}/(\dot{m}_{H_2O} + \dot{m}_{C_2H_5OH})$, where $\dot{m}_{H_2O}$ and $\dot{m}_{C_2H_5OH}$ are mass flow rates of water and ethanol, respectively, on the droplet surface (dotted line).
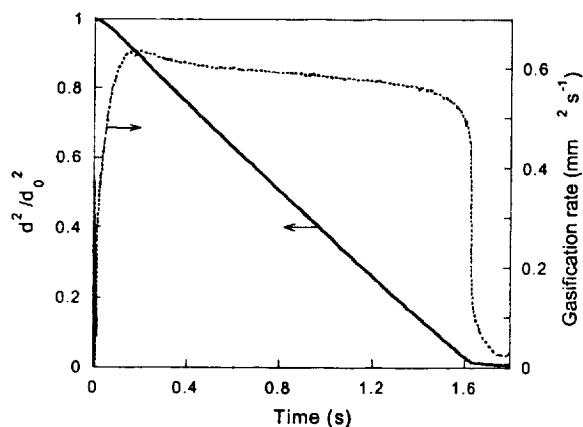

Figure 2. Computed diameter-squared normalized by initial diameter-squared (solid line) and instantaneous gasification rate (dotted line) for 1 mm ethanol droplet burning in air at 1 atm.
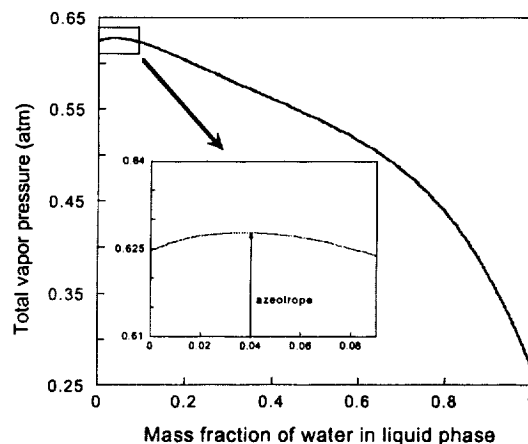

Figure 4. Total equilibrium vapor pressure above the liquid ethanol/water mixture as a function of water mass fraction in liquid phase at 340 K, a representative interface surface temperature predicted by the model.